Dense and Dynamic Polyethylene Glycol Shells Cloak Nanoparticles from Uptake by Liver Endothelial Cells for Long Blood Circulation

Hao Zhou[†], Zhiyuan Fan[†], Peter Y. Li[†], Junjie Deng[†,‡], Dimitrios C. Arhontoulis[⊥], Christopher Y. Li[†], Wilbur B. Bowne[§], and Hao Cheng[*,†,⊥]

[†]Department of Materials Science and Engineering, Drexel University, Philadelphia, Pennsylvania, 19104 USA

[‡]Engineering Research Center of Clinical Functional Materials and Diagnosis & Treatment Devices of Zhejiang Province, Wenzhou Institute of Biomaterials and Engineering, CAS, Wenzhou, 325011 China

[⊥]School of Biomedical Engineering, Science and Health Systems, Drexel University, Philadelphia, Pennsylvania, 19104 USA

[§]Department of Surgery, Drexel University, Philadelphia, Pennsylvania 19102, USA

* E-mail: hcheng@drexel.edu.

Supporting Information

Supporting information tables

Table S1. Pharmacokinetic parameters of PLGA-TPEG-NPs obtained by fitting the circulation data into one-compartment model via PKSolver. Values indicate mean ± SD (n = 6, from two independent experiments).

PLGA-PEG-MAL %	0	10	20	40	60	80	100
Clearance	0.22 ± 0.02	0.10 ± 0.01	0.07 ± 0.01	0.12 ± 0.02	0.18 ± 0.05	0.20 ± 0.03	0.22 ± 0.03
AUC 0-t	4.48 ± 0.48	10.1 ± 1.13	13.2 ± 0.86	8.82 ± 1.20	5.97 ± 1.75	5.07 ± 0.74	4.72 ± 0.83
AUC 0-inf	4.65 ± 0.57	10.2 ± 1.23	13.7 ± 0.97	8.90 ± 1.28	5.98 ± 1.77	5.07 ± 0.74	4.72 ± 0.83
AUMC (h^2)	23.8 ± 5.78	113 ± 28.9	199 ± 24.0	88.2 ± 27.7	42.2 ± 24.9	29.7 ± 7.21	26.0 ± 10.7
MRT	5.06 ± 0.55	10.9 ± 1.41	14.4 ± 0.75	9.70 ± 1.50	6.52 ± 1.83	5.77 ± 0.62	5.29 ± 1.20
Vss	1.09 ± 0.02	1.07 ± 0.03	1.06 ± 0.04	1.09 ± 0.04	1.09 ± 0.04	1.14 ± 0.07	1.11 ± 0.08

Table S2. Circulation half-lives of PLGA-TPEG-NPs obtained by fitting the circulation data into two-compartment model via PKSolver. Values indicate mean ± SD (n = 6, from two independent experiments).

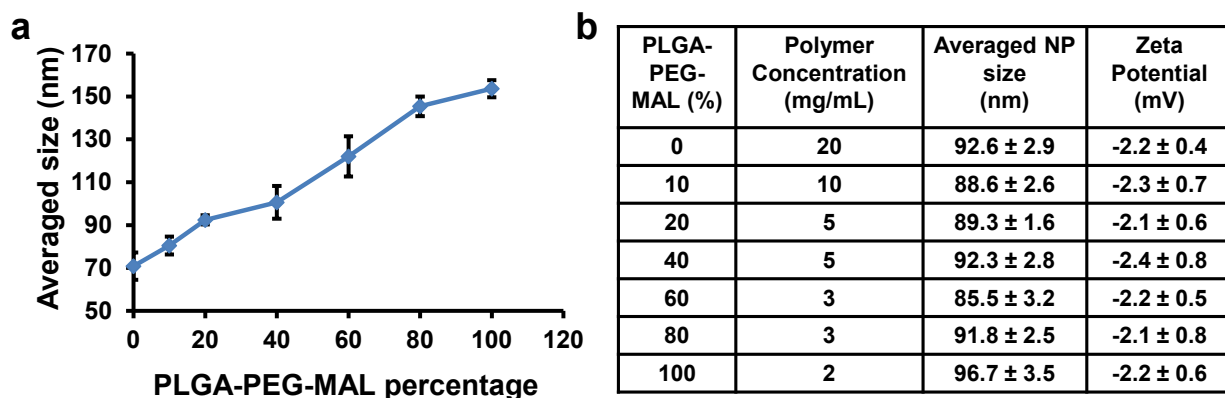| PLGA-PEG-MAL %	0	10	20	40	60	80	100
Distribution Half-life (h)	0.36 ± 0.12	1.67 ± 1.17	3.23 ± 3.95	1.26 ± 0.85	1.17 ± 0.68	1.02 ± 1.01	0.96 ± 0.75
Elimination Half-life (h)	4.90 ± 0.73	15.8 ± 4.82	13.20 ± 2.82	13.54 ± 2.40	13.24 ± 2.92	11.98 ± 5.66	10.51 ± 2.96

Table S3. Averaged sizes of PLA-TPEG-NPs prepared with different PLA-PEG-MAL ratios and total polymer concentrations. Values indicate mean ± SD (n = 3). The averaged sizes for NPs were controlled to be in a narrow range of 78-93 nm to minimize the effect of particle size on circulation.

| PLA-PEG-MAL (%)	Polymer Concentration (mg/mL)	Averaged NP size (nm)
0	30	81.8 ± 1.6
5	10	79.1 ± 4.5
10	8	84.4 ± 1.3
20	8	83.9 ± 4.0
40	5	78.3 ± 4.9
60	5	81.7 ± 3.9
80	3	86.7 ± 3.4
100	3	92.8 ± 10.8

Table S4. Calculated average distance between neighboring chains (D) and thickness (L) of the outer PEG layer of PLA-TPEG-NPs. The calculation followed a standard method using hydrated NP size from DLS to estimate NP concentration and surface area, and followed de Gennes' model of grafted polymers on a flat surface in a good solvent. In the mushroom regime ($D > R_F$) and mushroom-to-brush transition regime, the thickness of PEG chains L is approximately R_F. Values indicate mean ± SD (n = 3).

PLA-PEG-MAL %	5	10	20	40	60	80	100
D (nm)	4.9 ± 0.1	3.6 ± 0.1	2.8 ± 0.1	2.6 ± 0.1	2.4 ± 0.2	1.8 ± 0.2	1.7 ± 0.1
L (nm)	3.5	3.5	3.9 ± 0.1	4.1 ± 0.1	4.3 ± 0.2	5.4 ± 0.2	5.5 ± 0.1

Supporting information figures

| PLGA-PEG-MAL (%)	Polymer Concentration (mg/mL)	Averaged NP size (nm)	Zeta Potential (mV)
0	20	92.6 ± 2.9	-2.2 ± 0.4
10	10	88.6 ± 2.6	-2.3 ± 0.7
20	5	89.3 ± 1.6	-2.1 ± 0.6
40	5	92.3 ± 2.8	-2.4 ± 0.8
60	3	85.5 ± 3.2	-2.2 ± 0.5
80	3	91.8 ± 2.5	-2.1 ± 0.8
100	2	96.7 ± 3.5	-2.2 ± 0.6

Figure S1. Preparation and size characterization of PLGA-TPEG-NPs. (a) The size of PLGA-TPEG-NPs increased with the percentage of PLGA-PEG-MAL when the total polymer concentration was fixed. NPs were prepared with 0%, 10%, 20%, 40%, 60%, 80% and 100% PLGA-PEG-MAL under a fixed polymer concentration of 5 mg/mL. The NP sizes were detected using dynamic light scattering (DLS). Values indicate mean ± SD (n = 3). (b) Averaged sizes of NPs prepared with different PLGA-PEG-MAL ratios and total polymer concentrations. Values indicate mean ± SD (n = 3). The averaged sizes for NPs were controlled to be in a narrow range of 85-97 nm to minimize the effect of particle size on circulation.
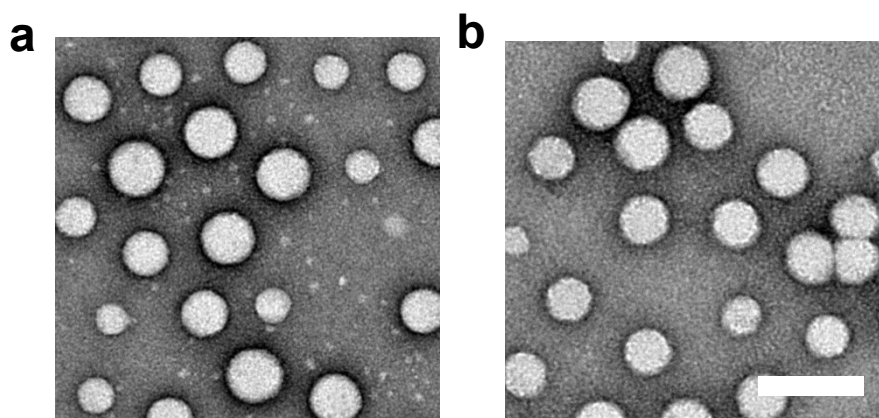

**Figure S2. TEM images of PLGA-PEG/TPEG-NPs.** (a) PLGA-PEG-NPs. (b) PLGA-TPEG-NP-100. (Scale bar: 100 nm)
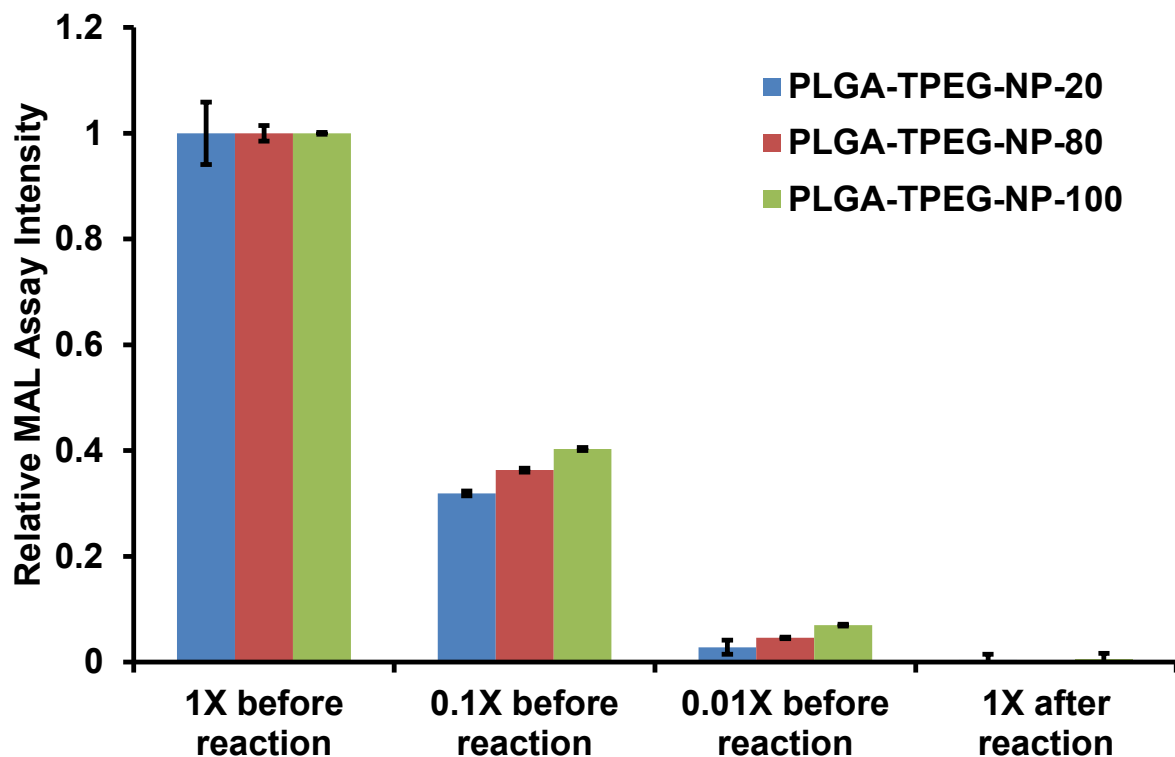
Figure S3. Characterization of the remaining maleimide on NP surfaces after the reaction with PEG$_{2K}$-thiol. MalemGreen Indicator, which has enhanced fluorescence upon reacting with a maleimide, was added to the solutions of NPs without PEG$_{2K}$-thiol conjugation (1X), their 10-fold dilutions (0.1X), 100-fold dilutions (0.01X), and solutions of NPs with PEG$_{2K}$-thiol conjugation. The concentrations of 1X solutions of PLGA-TPEG-NPs containing 20%, 80%, and 100% PLGA-PEG-MAL were 50, 20, and 20 mg/mL respectively to fit maleimide concentrations into the detection sensitive range. After the reaction, the remaining maleimide on NP surfaces was undetectable (<1%) suggesting a complete reaction (>99%) between maleimide on NP surfaces and PEG-thiol. Values indicate mean ± SD (n = 3).
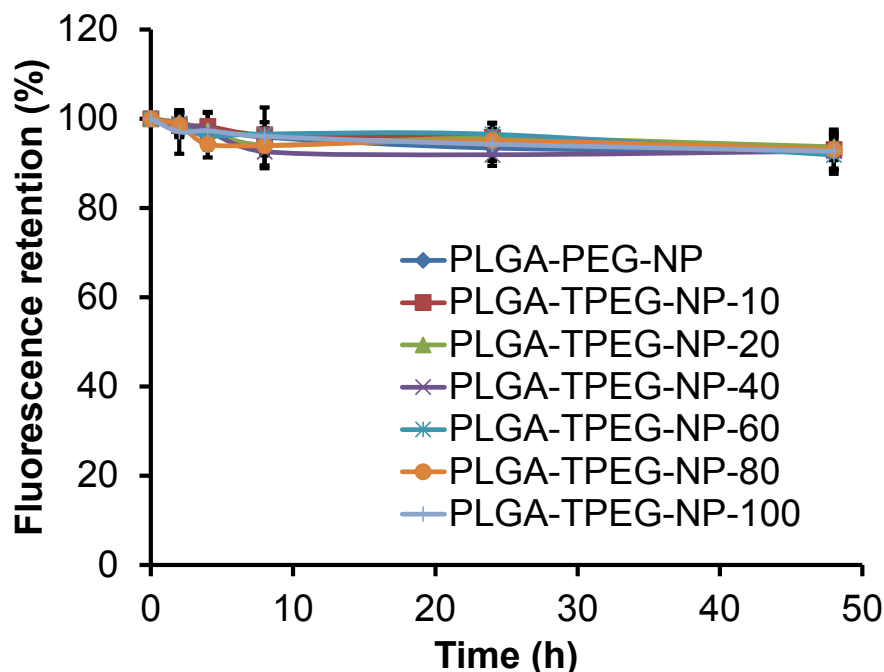
Figure S4. **Fluorescence retention of DiD-labeled PLGA-TPEG-NPs.** NPs in PBS supplemented with 10% FBS were shaken in a Slide-A-Lyzer dialysis device at 37 °C for 48 h and their fluorescence retention were measured via TECAN. Values indicate mean ± SD (n = 3).
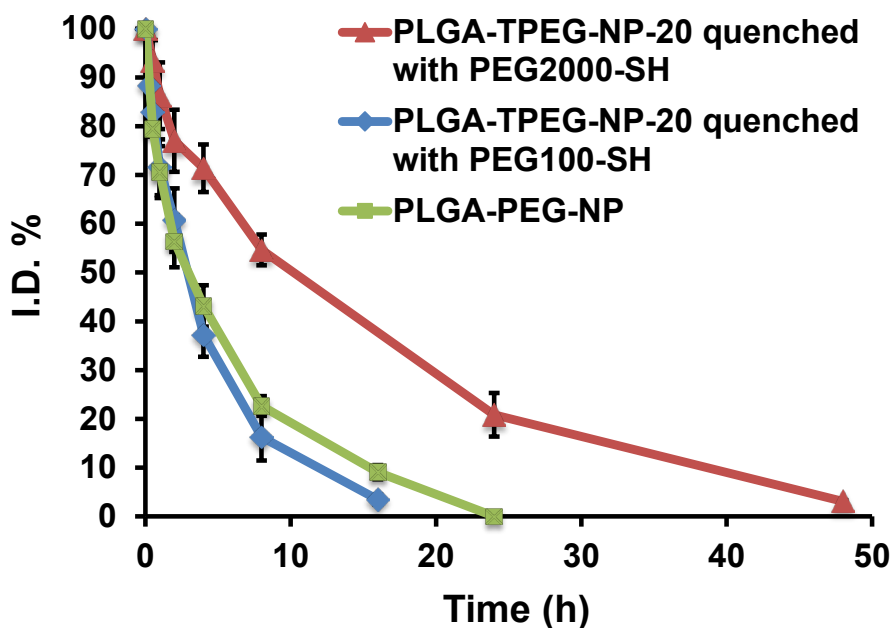
Figure S5. **Extended blood circulation of PLGA-PEG-NPs from a dynamic outer PEG layer instead of maleimide-thiol linkages.** *In vivo* blood circulation profiles of PLGA-TPEG-NP-20 quenched with thiol-PEG$_{2K}$ and thiol-PEG$_{100}$ and conventional PLGA-PEG-NPs. Value indicates mean ± SD (n = 3).
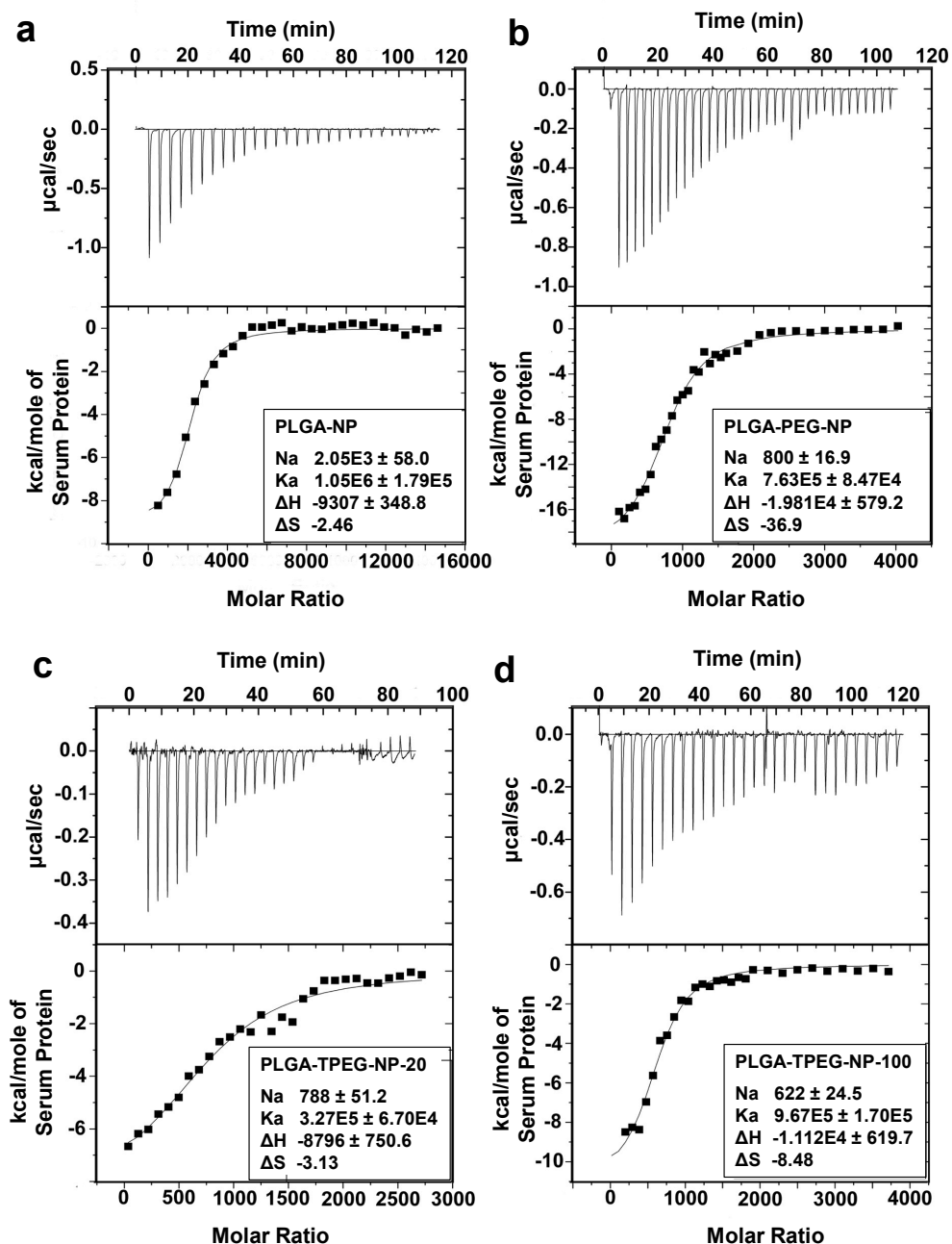
Figure S6. Original ITC data from the study of protein interaction with NPs. (a-d) Representative ITC data. Graphs show original power change for each titration over time and the integrated heat of each titration (n) with a corresponding fitted curve based on the one-site binding model of (a) PLGA-NPs, (b) PLGA-PEG-NPs, (c) PLGA-TPEG-NP-20 and (d) PLGA-TPEG-NP-100.
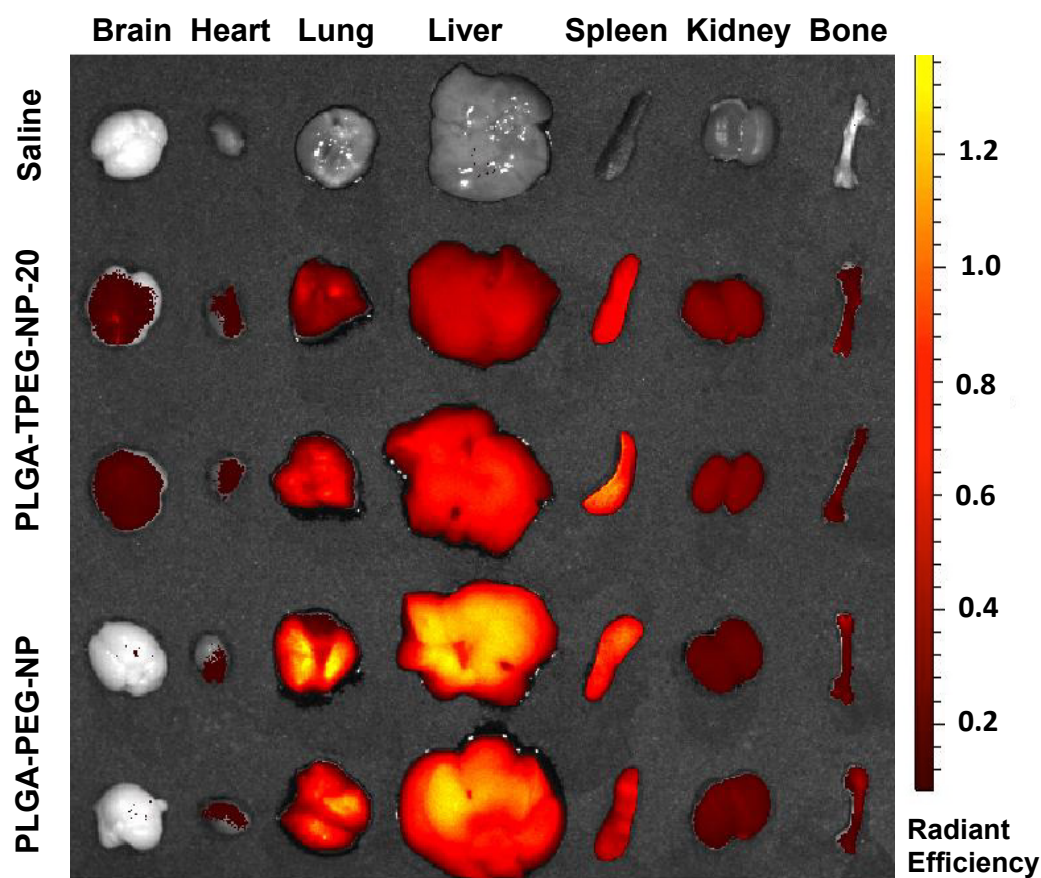
Figure S7. IVIS fluorescence image showing a dynamic topographical structure of outer PEG layer reduced NP uptake in the liver. IVIS fluorescence image of tissues at 4 h post tail vein injection of either PLGA-PEG-NPs or PLGA-TPEG-NP-20. The blood of mice were perfused with PBS immediately after euthanization and before the tissues were harvested. The NPs in the lungs may be from the remained blood due to the insufficient blood removal in the lungs after the air filling tissues collapsed in the perfusion process.
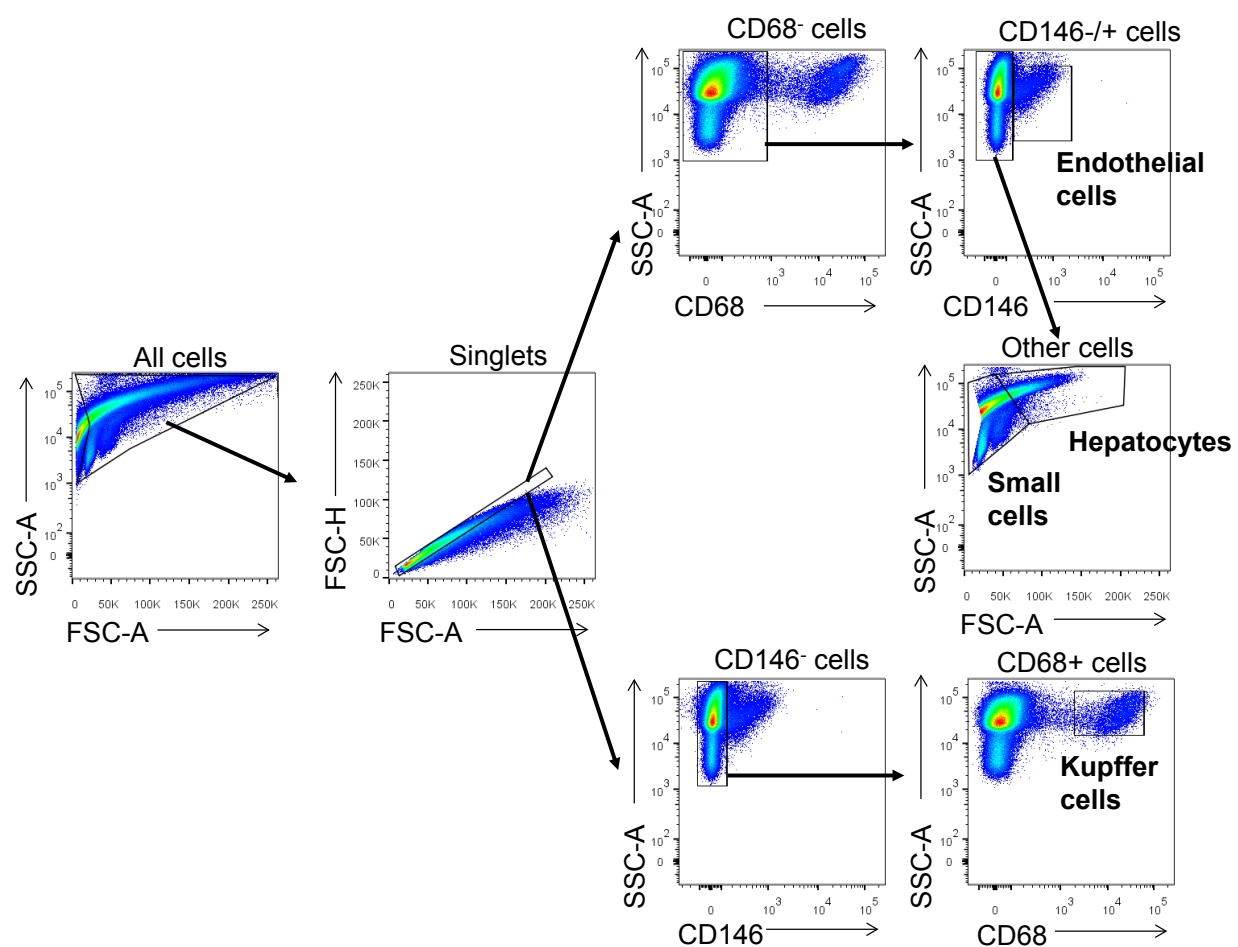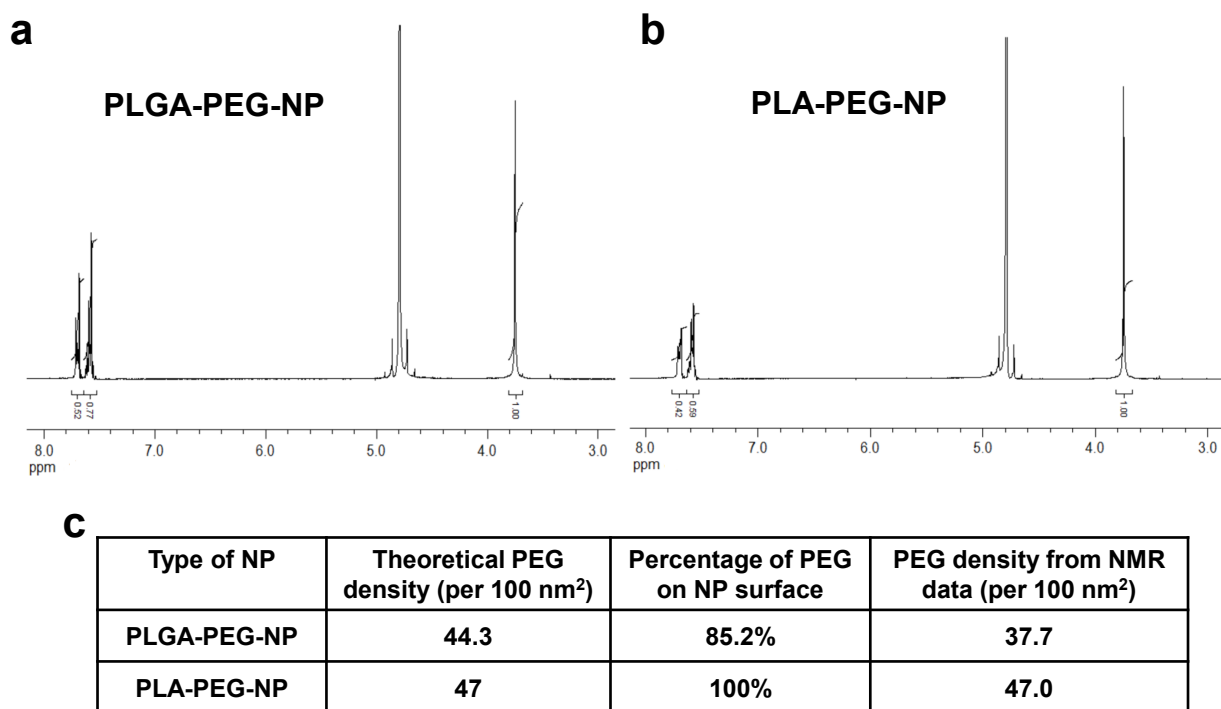
Figure S8: Liver cell gating strategy based on scatter of light and CD146/CD68 staining.
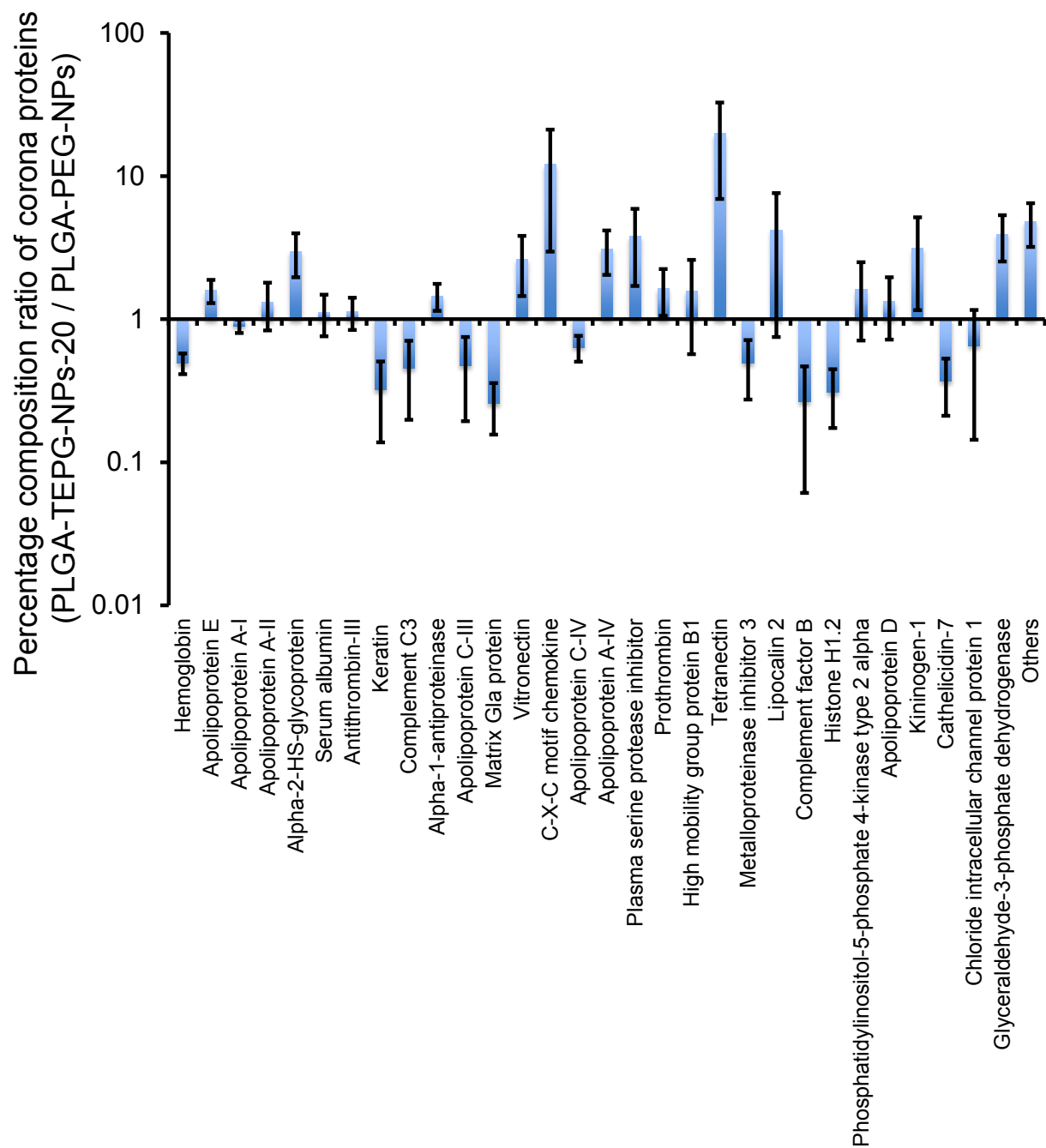
Figure S9. Variation of protein percentage composition in the corona of PLGA-PEG-NPs and PLGA-TPEG-NPs-20. Proteomic analysis of adsorbed proteins on NPs was performed using liquid chromatography-tandem mass spectrometry (LC-MS/MS). The most abundant 30 proteins in the protein corona of PLGA-PEG-NPs were identified. The percentage composition of these proteins were compared. When the ratio of a specific protein is higher than 1, it indicates the percentage of this protein is higher in PLGA-TPEG-NPs than in PLGA-PEG-NPs. Value indicates mean ± SD (n = 3).
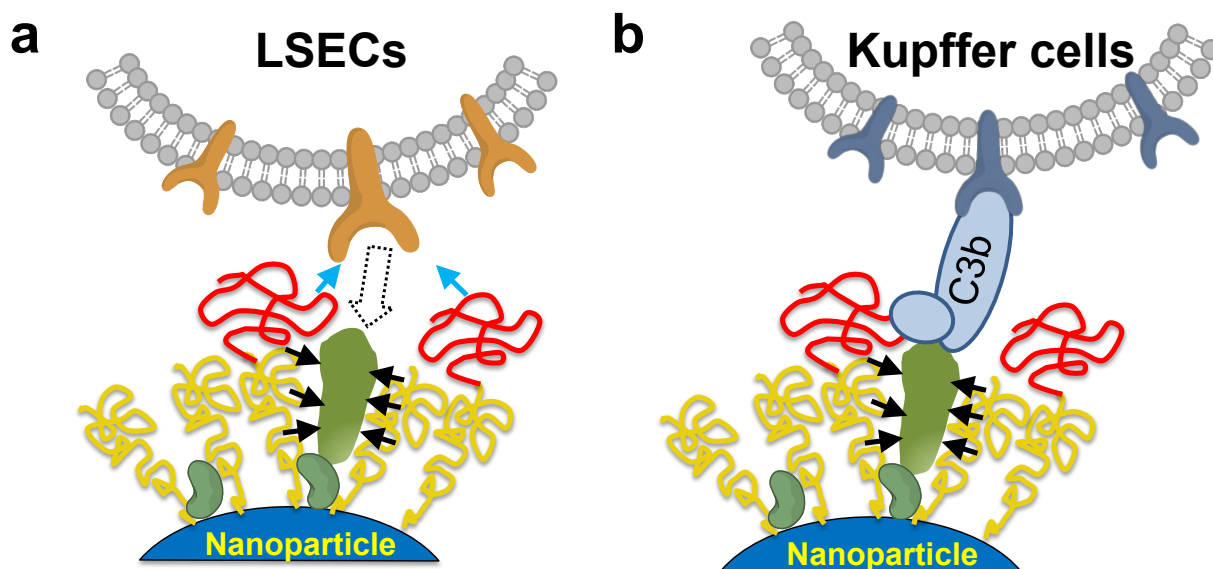
Figure S10. Illustration of proposed protein, cell receptor and PEG layer interactions. The outer PEG layer is marked in red. (a) Flexible PEG chains provide "entropic resistance" to proteins. There are spaces in the low density outer layer for chains to fluctuate, interfering with protein adsorption and the interactions between cell receptors and their protein ligands adsorbed on NPs. To penetrate into the primary PEG layer, proteins need to overcome the chain entropy loss. Black arrows indicate the resistance that proteins need to overcome to anchor on NP surfaces. Blue arrows indicate chain fluctuation interferes with the protein-receptor interactions. (b) Complement proteins, which have a high molecular weight, chemically link to adsorbed proteins. Their large sizes dwarf the effect of chain fluctuation.

a

PLGA-PEG-NP

b

PLA-PEG-NP

Type of NP	Theoretical PEG density (per 100 nm^2)	Percentage of PEG on NP surface	PEG density from NMR data (per 100 nm^2)
PLGA-PEG-NP	44.3	85.2%	37.7
PLA-PEG-NP	47	100%	47.0

Figure S11. NMR characterization of PEG chain density outside NPs. (a,b) ^{1}H-NMR spectrums of PLGA-PEG-NPs (a) and PLA-PEG-NPs (b) in D$_2$O. 6.6 mg PLGA-PEG-NPs and 6 mg PLA-PEG-NPs were prepared and dispersed in 0.7 mL D$_2$O. 5 mg of sodium benzenesulfonate was added into each sample as an external standard. (c) PEG chain density on NP surfaces. Theoretical estimation is based on the assumption that PEG chains are all on the outside of NPs. Experimental calculation is based on the NMR quantification of PEG chains on NP surfaces. The surface area and weight of each NP are estimated based on the size of NPs detected from DLS.